An insight into the unloading/reloading loops on the compression curve of natural stiff clays

Yu-Jun Cui, Xuan-Phu Nguyen, Anh Minh A.M. Tang, Xiang-Ling Li

An insight into the unloading/reloading loops on the compression curve of saturated clays

Cui Y.J.[1], Nguyen X.P.[1], Tang A.M.[1], Li X.L[2].

1 : Ecole des Ponts ParisTech, Laboratoire Navier/CERMES, 6 – 8 av. Blaise Pascal, Cité Descartes, Champs – sur – Marne, 77455 Marne – la – Vallée cedex 2, France

2 : Euridice Group, c/o SCK/CEN, Mol, Belgium

Corresponding author:

Prof. Yu-Jun CUI

Ecole des Ponts ParisTech

6-8 av. Blaise Pascal, Cité Descartes, Champs-sur-Marne

F-77455 MARNE LA VALLEE - France

Telephone : +33 1 64 15 35 50

Fax : +33 1 64 15 35 62

E-mail : yujun.cui@enpc.fr

Abstract

Oedometer tests were carried out with loading/unloading/reloading on natural saturated Ypresian clay taken from several depths. Common unloading/reloading loops were identified. Further examination of the unloading or reloading curves shows that each path can be satisfactorily considered as bi-linear with a small and a larger slopes separated by a threshold vertical stress. This threshold stress can be considered as the swelling pressure corresponding to the void ratio just before the unloading or reloading. Indeed, upon unloading, when the applied stress is higher than the threshold stress or swelling pressure, the mechanical effect is dominant and only small mechanical rebound is observed, corresponding to a small microstructure change; by contrast, when the applied stress is lower than the swelling pressure, physico-chemical effect becomes prevailing, and soil swelling occurs with a larger microstructure change. Upon reloading, when the applied stress is lower than the swelling pressure, the microstructure is not significantly affected thanks to the contribution of the physico-chemical repulsive force, leading to a small volume change; on the contrary, beyond the swelling pressure, the mechanical effect becomes dominant giving rise to larger volume change corresponding to the microstructure collapse. Like unsaturated expansive soils, it is found that there is a good relationship between the swelling pressure (threshold stress) and the void ratio just before the unloading or reloading. This is confirmed by the results from the data reported in the literature on Boom and London clays. It can be then deduced that the unloading/reloading loop is rather due to the competition between the mechanical and physico-chemical effects on the microstructure changes than the viscosity effect as commonly admitted.

Keywords: clays; unloading/reloading loops; oedometer tests; mechanical effect, physico-chemical effect; swelling pressure.

Introduction

It is well known that the soil compression curves show unloading/reloading loops. These loops have been commonly explained by the soil viscosity effect: clayey soils have larger loops because of their relatively higher viscosity, and sandy soils have narrow loops because of their low viscosity, silty soils being in between. Indeed, Coop & Lee (1993) performed compression tests on the Ham River sand and Dogs bay sand, and the results from unloading/reloading paths show a negligible hysteresis without any marked loops. However, the unloading/reloading loop is quite clear for silty soils (see Nasreddine 2004 for instance), and becomes much more marked for clayey soils (Holtz et al. 1986), bentonite (Borgesson et al. 1996), bentonite/sand mixtures (Tong & Yin 2011), kaolin/bentonite mixture (Di Maio et al. 2004), and claystone (Mohajerani et al. 2011). When investigating the compressibility of a soil, these loops are often ignored and an average slope is usually considered in the calculation of soil volume change. Obviously, this practice is relatively easy for sandy soils and silty soils, but difficult for clayey soils and even impossible for expansive soils.

From a foundamental point of view, explaining the unloading/reloading loops by viscosity effect seems too simplistic and unclear. Further study on the corresponding mechanisms is needed. But to the authors' knowledge, there is up to now no plausible mechanisms developed allowing correctly explaining the soil volume change behaviour under unloading/reloading. In this study, this aspect was investigated by performing oedometer tests with several unloading/reloading cycles on natural Ypresian stiff clays. The results were analysed based on the competition between the mechanical effect and physico-chemical effect occurred during unloading or reloading. A new mechanism related to the soil swelling pressure was proposed. This mechanism was verified by the results from the oedometer tests on other natural stiff clays such as Boom clay and London clay.

Materials and methods

The materials studied are cores sampled from Ypresian formation at four different depths, namely YP43 from 330.14 m - 330.23 m depth, YP64 from 351.20 m - 351.29 m depth, YP 73 from 361.30 m- 361.34 m depth, and YP95 from 382.35 m - 382.44 m depth. Their clay mineralogy and physical properties are shown in Table 1 and Table 2, respectively. The four depths have comparable clays fraction (between 48 and 59%) as well as similar smectite content (between 26 and 34%), suggesting similar physical properties in terms of plasticity. However, the values of plasticity index I_p and methylene blue VBS (see Table 2) shows a much lower plasticity of YP43 as compared to the three other depths. YP43 has also the lowest liquid limit (w_L = 75) and the highest carbonates content $CaCO_3$ (10.16%), its other parameters (specific gravity G_s, plastic limit w_P, initial water content w_0, initial void ratio e_0) being similar to that of other depths. It is possible that the high carbonates content of YP43 gives rise a lower level of plasticity as indicated by the values of I_p and VBS in Table 2. Further study is needed to clarify this point.

Oedometer tests were performed on soil samples of 50-mm diameter and 20-mm height by hand-trimming from cores that have 1000-mm length and 100-mm diameter. After installing soil sample in the oedometer cell, step loading up to the in situ vertical effective stress (up to point A in Figure 1a) was carried out without contact with water in order to avoid any swelling which would affect the initial soil microstructure (Delage et al., 2007; Cui et al. 2009, Deng et al., 2011a, 2011b, 2011c). Note that the in-situ vertical effective stresses (σ'_{v0}) were estimated by taking an average mass density of overburden soils equal to 1.9 Mg/m^3 (Van Marcke & Laenen, 2005) with an underground water level assumed to be at the ground surface. For a reason of convenience, σ'_{v0} were rounded to 3.2 MPa for all the four depths.

The degree of saturation at point A, calculated using the initial degree of saturation (see S_{r0} in Table 2) and the volume change recorded, was found to be 100% for all samples tested.

Under σ'_{v0}, the bottom porous stone and the drainage tubes were saturated with the in-situ synthetic water that has the same chemical composition as the field water (A-B). Afterwards, step unloading to 0.125 MPa (B-C), reloading up to 16 MPa (C-D), unloading again to 0.125 MPa (D-E), reloading up to 32 MPa (E-F) and finally unloading to 0.125 MPa (F-G) were conducted. The stabilization of volume change was considered as achieved when the vertical strain rate is lower than 5×10^{-4}/8 h (AFNOR, 1995, 2005).

Test results

Figure 1 shows the compression curve for the four depths. For YP43 (Figure 1a), YP64 (Figure 1b) and YP73 (Figure 1c), two full unloading/reloading cycles and one extra single unloading were applied, while for YP95 (Figure 1d), only one full cycle and one extra single unloading were applied. Figure 1a shows that the application of the in-situ vertical stress (3.2 MPa) led the soil sample to point A. When saturating the bottom porous stone and the drainage tubes, a negligible volume change (A to B) was observed, confirming that the sample was fully saturated. Upon unloading from B to C, a nearly bi-linear curve was observed: when the stress was higher than a threshold stress σ_{s1} the slope was small, and when the stress was lower than σ_{s1} the slope is significantly larger. Upon reloading from C to D, a tri-linear curve was identified. Below the stress at point B, a nearly bi-linear curve was again observed, with a small slope below a threshold stress σ_{s4} and a larger slope beyond σ_{s4}. Further loading beyond point B gave rise to a larger slope, certainly related to the plastic volume changes. Examination of the unloading/reloading curve B-C-B shows a hysteretic

loop. The same phenomenon can be observed when unloading the sample from D to E and reloading the sample from E to F: there is a nearly bi-linear curve from D to E with a small slope beyond a threshold stress σ_{s2} and larger slope below σ_{s2}, there is also a nearly bi-linear curve from E to D with a threshold stress σ_{s3}, and when the stress is beyond point D, the slope is increased because of the plastic volume change. The unloading from F to G confirmed the bi-linearity of the curve with a threshold stress σ_{s3}. Comparison of the unloading slopes shows that both the small slope and large slope were increasing with the maximum stress applied prior to unloading.

The same observation can be made on the results from the tests on the other three depths (YP64 – Figure 1b, YP73 – Figure 1c and YP95 – Figure 1d). There are also more or less well defined bi-linear curves for both unloading and reloading paths with threshold stresses.

It must be mentioned that the bi-linearity observed in this study should be considered as a particular case because for most soils non-linear curves are often observed. It is likely that there is relatively well defined bi-linearity for natural stiff clays like the studied natural Ypresian clay. Basically, the shape of the curves depends on both the soil nature and soil microstructure.

To further analyse the results, in Figure 2, the values of threshold stress in Figure 1 for each depth are presented as a function of the void ratio just before each unloading or reloading (σ_{s1} with $e_{i1;}$ σ_{s2} with $e_{i2;}$ σ_{s3} with $e_{i3;}$ σ_{s4} with $e_{i4;}$ σ_{s5} with e_{i5}). A good linear relationship is obtained in a semi-logarithmic plane for all the four depths. In order to verify this observation, some results from oedometer tests on other stiff clays from the literature are collected, and shown in Figure 3 together with the results of Ypresian clay. It is observed that the variations of swelling pressure with the initial void ratio before unloading or reloading for Boom clay from Essen taken at different depths (Ess 75, Ess 83, Ess 96, Ess 104, Ess112) and

for Boom clay from Mol (Deng et al. 2011a, Horseman et al. 1987) show also good linear functions. Obviously, the relationship between σ_s and e_i is soil nature dependent: the slope is different for different soils.

Figure 4 shows the results obtained on the basis of the data reported by Gasparre and Coop (2008) on London clay at Healthrow Airport Terminal 5. It involves six samples from different depths: 7 m (C7), 10 m (B10), 25 m (B25), 28 m (B28), 36 m (A36) and 51 m (A51). Again, a good linear relationship is observed for all samples with unloading/reloading.

Interpretation and discussion

Delage and Lefebvre (1984) showed that when compressing a clayey soil in oedometer, macro-pore collapse occurs first during loading path under stresses higher than the preconsolidation pressure or yield stress of soil, leading to irrecoverable volume changes; this process results in microstructure changes characterized by more and more orientated particles. As Le et al. (2011) indicated with a more orientated microstructure the physico-chemical interaction between clay particles and adsorbed water is enhanced. Indeed, Olson and Mesri (1970) pointed out that the competition between the mechanical effect and physico-chemical effect on soil volume change behaviour depends strongly on the particles geometric arrangement defined by the contact angle between particles: the mechanical effect is more pronounced when the contact angle is large, and on the contrary, the physico-chemical effect becomes dominant when the particles are more parallel with a small contact angle. Thereby, upon mechanical loading in oedometer the contact angle is decreasing, leading to increase of the physico-chemical effect.

Basically, the increase of physico-chemical effect due to loading can be well evidenced during unloading: the more oriented particles undergo higher repulsion forces and thus show more significant swell: the unloading curve could have a much greater slope than the initial

loading slope before the preconsolidation pressure is reached, and the void ratio after full unloading could even be higher than the initial void ratio. Examination of the unloading slopes in Figure 1 confirms this reasoning: the unloading slope is indeed increasing with increasing yield stress.

The description above shows that when unloading from the previous maximum stress (commonly termed as yield stress), the compression behaviour is mainly governed by the competition between the physico-chemical effect and mechanical effect. When the external stress is higher than the repulsive force related to the soil particles-water interaction (physico-chemical effect), low swelling volume change occurs; otherwise higher swelling volume change can be expected. Similarly, upon reloading, when the external stress is lower than the repulsive force related to the physico-chemical effect, this external stress is balanced by the repulsive force, leading to a small volume decrease; on the contrary, when the external stress becomes higher, the mechanical effect becomes dominant giving rise to larger volume decrease. This conceptual description implies that it is possible to determine some characteristic stress that separate the zone with prevailing physico-chemical effect from the zone with prevailing mechanical effect. It is indeed what is observed in Figure 1 with the threshold stress. Upon unloading, when the vertical stress is higher than the threshold stress σ_s, the volume change is characterized by the mechanical rebound; however, in the lower stress range the volume change is characterized by the physico-chemical swelling.

Furthermore, if we admit that the physico-chemical effect mentioned above corresponds to the matric suction as we do commonly for expansive soils (saturated or unsaturated), the threshold stress identified should correspond to the swelling pressure. Indeed, the swelling pressure of a soil is commonly defined as the stress under which no volume change occurs upon wetting. According to this definition, swelling takes place when wetting a soil under a

191 stress lower than the swelling pressure; on the contrary, collapse takes place when wetting the
192 soil under a stress higher than the swelling pressure. Thus, the swelling pressure can
193 experimentally be determined by loading the soil samples in oedometer to different vertical
194 stress σ_v' and then wetting them (see Figure 5a). Various other methods can be used for this
195 purpose (see Figure 5b). The "constant-volume" method (path OA) is based on the use of a
196 relatively rigid cell with total pressure measurement (Tang et al., 2011, Wang et al. 2012).
197 The value of pressure after stabilisation is the swelling pressure of soil. For the "zero-swell"
198 method (path OBB') the equipment employed is a conventional oedometer (Basma et al.,
199 1995; Nagaraj et al., 2009). Firstly, a low initial load (0.1 MPa for example) is applied on the
200 specimen prior to water flooding. As the specimen wets up it attempts to swell. When the
201 swell exceed a certain value (0.1% for example), additional pressure is added in small
202 increment to bring the volume of soil specimen back to its initial value (Basma et al., 1995;
203 Attom et al., 2001). This operation is repeated until the specimen ceases to swell. The
204 swelling pressure is defined as the stress under which no more swelling occurs. The "swell-
205 consolidation" method (path OCC') consists of re-saturating the soil under a low pressure (0.1
206 MPa for example). After swell completion, standard consolidation test is performed. The
207 pressure required to bring the soil specimen back to its original void ratio is defined as the
208 swelling pressure (Basma et al., 1995; Agus, 2005).

209 The small mechanical rebound upon unloading implies an insignificant microstructure
210 change, i.e., the microstructure pattern remains rather orientated with dominated face-to-face
211 particle contacts (see Figure 6). When the external stress is lower than the threshold stress or
212 swelling pressure σ_s, the prevailing physico-chemical effect leads to a significant
213 microstructure change characterized by formation of more and more face-to-edge particle
214 contacts. This microstructure change corresponds to a larger soil swelling. From this
215 description, the threshold stress or swelling pressure σ_s separates the zone with insignificant

microstructure change from the zone with significant microstructure change. The increase of this swelling pressure with loading ($\sigma_{s1} < \sigma_{s2} < \sigma_{s3}$) observed in Figure 1 is also consistent with the common results on unsaturated expansive soils: a higher stress causes lower void ratio or higher density, increasing the swelling pressure (Villar et al., 2008; Siemens et al., 2009; Wang et al., 2012).

The reasoning above applies also for the reloading path. When the external stress is lower than the swelling pressure, the matric suction related to the physico-chemical effect is high enough to balance the effect of external stress, and the current microstructure changes insignificantly (with the face-to-edge particles preserved). As a result, the slope of the compression curve is small. By contrast, when the external stress is higher than the swelling pressure, the mechanical effete becomes dominant and larger volume change occurs by collapse of large-pores (the particles arrangement tends towards face-to-face type), leading to a larger slope of the compression curve. This is also consistent with the swelling pressure definition shown in Figure 5.

It should be mentioned that the model used above for microstructure changes during unloading/reloading is totally conceptual. It should be confirmed by experimental evidences provided in further studies implying appropriate techniques. Theoretically, the more plastic the soil is (high smectite content, high plasticity index I_p, large methylene blue value, etc.), the more microstructure changes from face-to-face pattern to face-to-edge pattern can be expected.

Figures 2-4 show that there is a linear relationship between swelling pressure and the void ratio before unloading or reloading in a semi-logarithmic scale for natural stiff clays as Ypresian clay, Boom clay and London clay, although this relationship is soil nature dependent. This is consistent with the results from the tests on unsaturated expansive soils,

thereby bring another evidence for the identified threshold stress as swelling pressure. Note that for other soils there is not necessarily bi-linear unloading/reloading curves, thus, difficult to determine the relationship between the swelling pressure and void ratio before unloading or reloading. However, it is believed that the conceptual model developed in this study would be still applicable.

Conclusion

Oedometer tests were carried out with loading/unloading/reloading on saturated natural Ypresian clay from different depths. The unloading/reloading loops of compression curves of Ypresian clay have been explained by the competition between the mechanical and physico-chemical effects. Upon unloading, when the applied stress is higher than the swelling pressure, the mechanical effect is dominant and only small mechanical rebound is observed; by contrast, when the applied stress is lower than the swelling pressure, physico-chemical effect becomes dominant, giving rise to soil swelling with a larger slope. Upon reloading, when the applied stress is lower than the swelling pressure, the microstructure is more or less preserved thank to the contribution of the matric suction, leading to a small volume change; on the contrary when the applied stress is higher than the swelling pressure, the mechanical effect prevails and larger volume change occurs by collapse of large-pores. The good linear relationship between the swelling pressure and the void ratio just before unloading or reloading confirms this interpretation. Further examination of Boom clay from both Essen and Mol sites as well as London clay brings further confirmation to this concept. It can be then concluded that the unloading/reloading loop is rather due to the competition between the mechanical and physico-chemical effects than the viscosity effect as commonly admitted. Note however that this interpretation was done only based on the oedometer tests on natural

263 stiff clays. Further studies are needed to make more clarification, especially in terms of
264 microstructure investigation.

265

266 **References**

267 AFNOR, 1995. Sols : reconnaissance et essais: essai de gonflement à l'oedomètre,
268 détermination des déformations par chargement de plusieurs éprouvettes. XP P 94-091.

269 AFNOR, 2005. Geotechnical investigating and testing, Laboratory testing of soils, Part 5:
270 Incremental loading Oedometer test. XP CEN ISO/TS 17892-5.

271 Agus, S., 2005. An Experimental study on hydro-mechanical characteristics of compacted
272 bentonite-sand mixtures. PhD thesis. Weimar.

273 Attom, M., Abu-Zreig, M. & Obaidat, M., 2001. Changes in clay swelling and shear strength
274 properties with different sample preparation techniques. Geotechnical Testing Journal,
275 ASTM, 24, 157-163.

276 Basma,A.A., Al-Homoud, A.S., Husein, A., 1995. Laboratory assessment of swelling
277 pressure of expansive soils. Applied Clay Science, 9(5), 355–368.

278 Borgesson, L., Karnland, O., Johannesson, L. E., 1996. Modelling of the physical behaviour
279 of clay barriers close to water saturation. Engineering Geology, 41, 127-144.

280 Coop, M. R., Lee, I. K., 1993. The behaviour of granular soils at elevated stresses. Proc.
281 Wroth Memorial Symposium: Predictive soil mechanics, pp. 186 - 198.

282 Cui Y.J., Le T.T., Tang A.M., Delage P., Li X.L., 2009. Investigating the time dependent
283 behaviour of Boom clay under thermo-mechanical loading. Géotechnique, 59 (4), 319-
284 329.

285 Delage P., Lefebvre G., 1984. Study of the structure of a sensitive Champlain clay and of its
286 evolution during consolidation. Canadian Geotechnical Journal, 21 (1), 21-35.

287 Delage P., Le T.T., Tang A.M., Cui Y.J., Li X.L., 2007. Suction and in-situ stresses of deep
288 Boom clay samples. Géotechnique, 57(1), 239-244.
289 Deng Y. F., Tang A. M., Cui Y. J., Nguyen X. P., Li X. L., Wouters L., 2011*a*. Laboratory
290 Hydro-mechanical Characterisation of Boom Clay at Essen and Mol. Physics and
291 Chemistry of the Earth, 36 (17-18), 1878–1890.
292 Deng Y.F., Tang A.M., Cui Y.J., Li X.L., 2011*b*. A study on the hydraulic conductivity of
293 Boom clay. Canadian Geotechnical Journal, 48, 1461-1470.
294 Deng Y. F., Cui Y. J., Tang A. M., Nguyen X. P., Li X. L., Van Geet M., 2011*c*. Investigating
295 the pore-water chemistry effects on the volume change behaviour of Boom clay. Physics
296 and Chemistry of the Earth, 36 (17-18), 1905–1912.
297 Di Maio, C., Santoli, L., Schiavone, P., 2004. Volume change behaviour of clays: the
298 influence of mineral composition, pore fluid composition and stress state. Mechanics of
299 Materials, 36, 435–451.
300 Gasparre, A., Coop, M. R., 2008. Quantification of the effects of structure on the compression
301 of a stiff clay. Canadian Geotechnical Journal, 45(9), 1324-1334.
302 Holtz, R. D., Jamiolkowski, M. B., Lancellotta, R., 1986. Lessons from oedometer tests on
303 high quality samples. Journal of Geotechnical Engineering, 112(8), 768-776.
304 Horseman, S.T., Winter M.G., Entwistle D.C., 1987. Geotechnical characterization of Boom
305 clay in relation to the disposal of radioactive waste. Commission of the European
306 Communities, EUR 10987, 87 p.
307 Le T.T., Cui Y.J., Munoz J.J., Delage P., Tang A.M., Li X., 2011. Studying the stress-suction
308 coupling in soils using an oedometer equipped with a high capacity tensiometer. Front.
309 Archit. Civ. Eng.China, 5(2), 160–170.
310 Mohajerani M., Delage P., Monfared M, Tang A.M., Sulem J., Gatmiri, B. 2011. Œdometer
311 compression and swelling behaviour of the Callovo-Oxfordian argillite. International

312 Journal of Rock Mechanics and Mining Sciences, 48(4), 606 – 615.
313 (doi:10.1016/j.ijrmms.2011.02.01)
314 Nagaraj, H. MOHAMMED Munnas, M. Sridharan,A., 2009. Critical Evaluation of
315 Determining Swelling Pressure by Swell-Load Method and Constant Volume Method,
316 Geotechnical Testing Journal, ASTM, 32, 305-314.
317 Nasreddine, K. 2004. Effet de la rotation des contraintes sur le comportement des sols
318 argileux. PhD thesis, Ecole Nationale des Ponts et Chaussées, Paris.
319 Olson R. O., Mesri G., 1970. Mechanisms controlling compressibility of clays. Journal of Soil
320 Mechanics and Foundation Division, Proceeding of the American Society of Civil
321 Engineers. SM6, pp. 1863-1878
322 Siemens, G., Blatz, J.A., 2009. Evaluation of the influence of boundary confinement on the
323 behaviour of unsaturated swelling clay soils. Canadian Geotechnical Journal, 46(3), 339–
324 356.
325 Tang C. S., Tang A. M., Cui Y. J., Delage P., Sshroeder C., De Laure E., 2011. Investigating
326 the Swelling Pressure of Compacted Crushed-Callovo-Oxfordian Argillite. Physics and
327 Chemistry of the Earth, 36 (17-18), 1857–1866.
328 Tong, F., Yin, J. H., 2011. Nonlinear Creep and Swelling Behavior of Bentonite Mixed with
329 Different Sand Contents Under Oedometric Condition. Marine Georesources &
330 Geotechnology, 29(4), 346-363.
331 Vandenberghe N., 2011. Qualitative & quantitative mineralogical analyses on the Ypresian
332 clay. Report of Applied Geology & Mineralogy Group of K. U. Leuven to NIRAS-
333 ONDRAF.
334 Van Marcke Ph., Laenen B. 2005. The Ypresian clays as possible host rock for radioactive
335 waste disposal: an evaluation. Report of Belgian agency for radioactive waste and
336 enriched fissile materials, 149p.

337 Villar, M.V., Lloret, A., 2008. Influence of dry density and water content on the swelling of a
338 compacted bentonite. Applied Clay Science, 39(1-2), 38–49.
339 Wang Q., Tang A.M., Cui Y.J., Delage P., Gatmiri B. 2012. Experimental study on the
340 swelling behaviour of bentonite/claystone mixture. Engineering Geology, 124, 59-66.
341

List of Tables

List of Figures

363

364 **Table 1. Mineralogy of Ypresian clay (Vandenberghe et al., 2011)**

Mineral	YP43	YP64	YP73	YP95
Depth (m)	330.14-330.23	351.20-351.29	361.30-361.34	382.35-382.44
Σ**Clay** (% wt)	**54**	**48**	**57**	**59**
Illite	5	4	5	6
Kaolinite	2	5	3	3
Smectite	32	26	33	34
Illite/Smectite	12	10	12	13
Chlorite/others	3	3	4	3
Σ**Non-clay** (% wt)	**46**	**52**	**43**	**41**
Quartz	32	36	31	27
K-feldspar	6	7	6	7
Plagioclase	6	6	5	3
Others	2	3	1	4

365

366 **Table 2. Physical properties of Ypresian clay**

Soil	G_s (-)	w_L (-)	w_P (-)	I_P (-)	w_0 (%)	e_0 (-)	S_{r0} (%)	VBS (g/100g)	$CaCO_3$ (%)
YP43	2.78	75	34	42	26	0.81	89	3.95	10.16
YP64	2.79	114	34	80	26	0.79	92	7.09	1.38
YP73	2.80	137	36	101	31	0.94	93	13.12	0.88
YP95	2.80	132	44	88	30	0.95	87	12.72	3.82

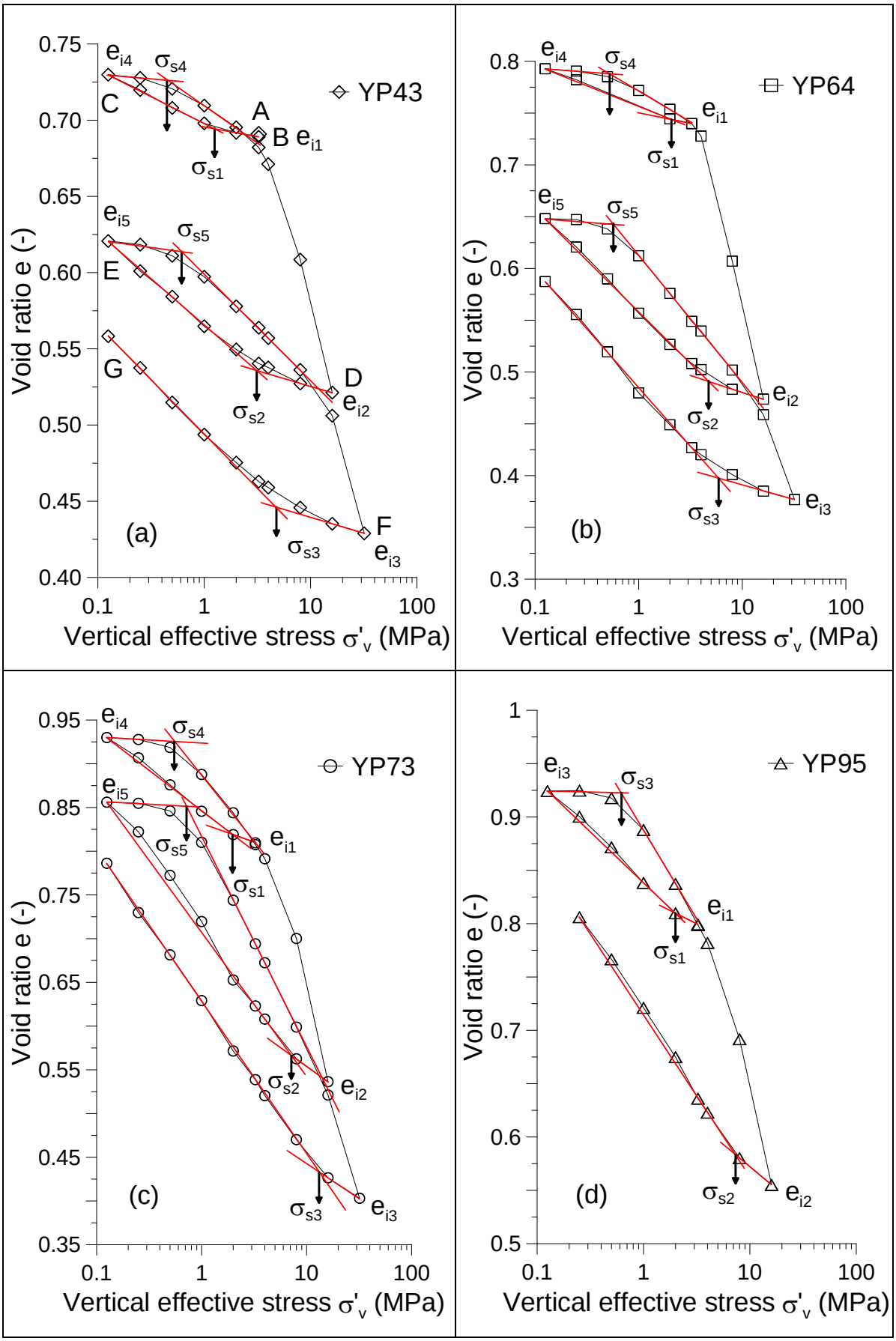

368 Figure 1. Oedometer test with unloading/reloading on Ypresian clays

369

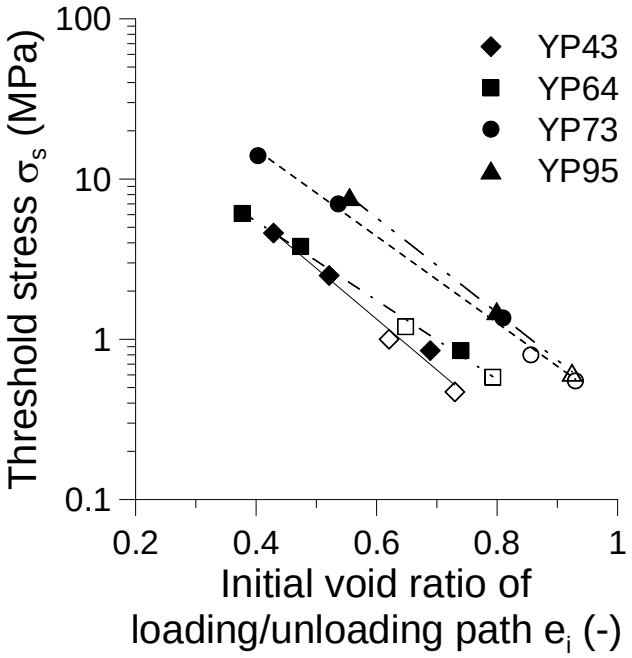

Figure 2. Swelling stress versus the void ratio just before unloading or reloading for Yprecian clays - Closed symbols are for unloading path, open symbols for loading path

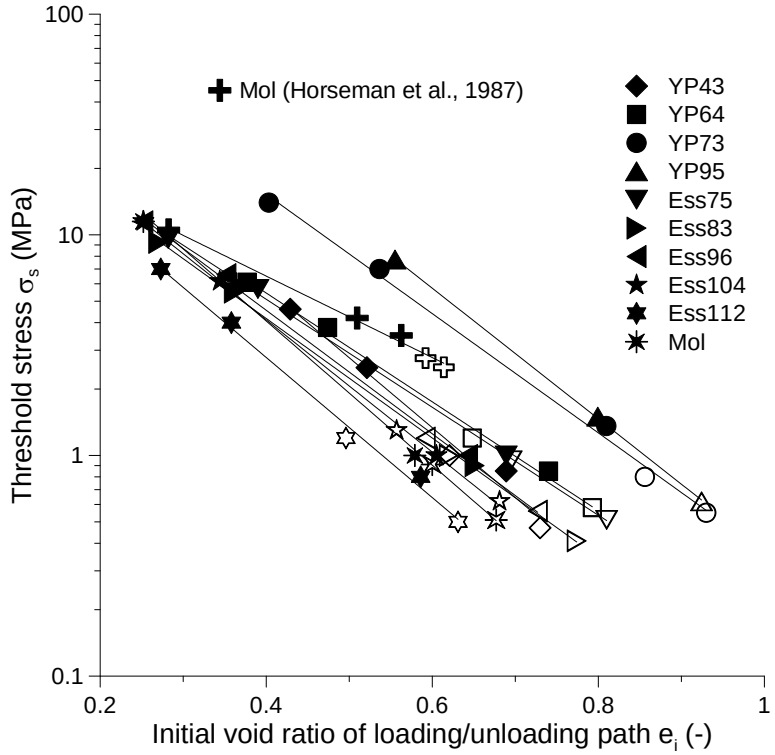

Figure 3. Swelling stress versus the void ratio just before unloading or reloading for Boom (from both Essen and Mol sites) and Ypresian clays. - Closed symbols are for unloading path, open symbols for loading path

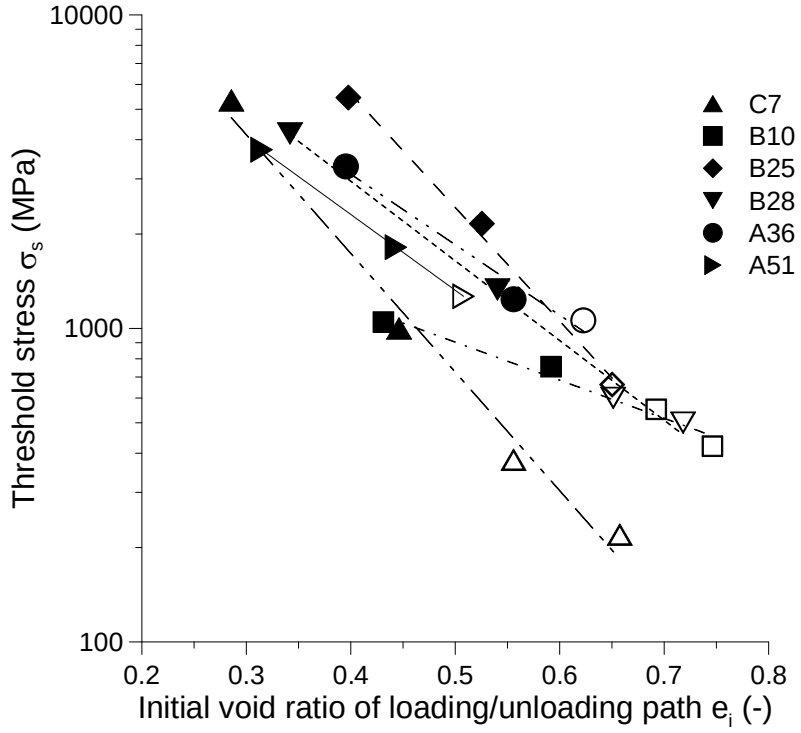

Figure 4. Swelling stress versus the void ratio just before unloading or reloading for London clay. - Closed symbols are for unloading path, open symbols for loading path

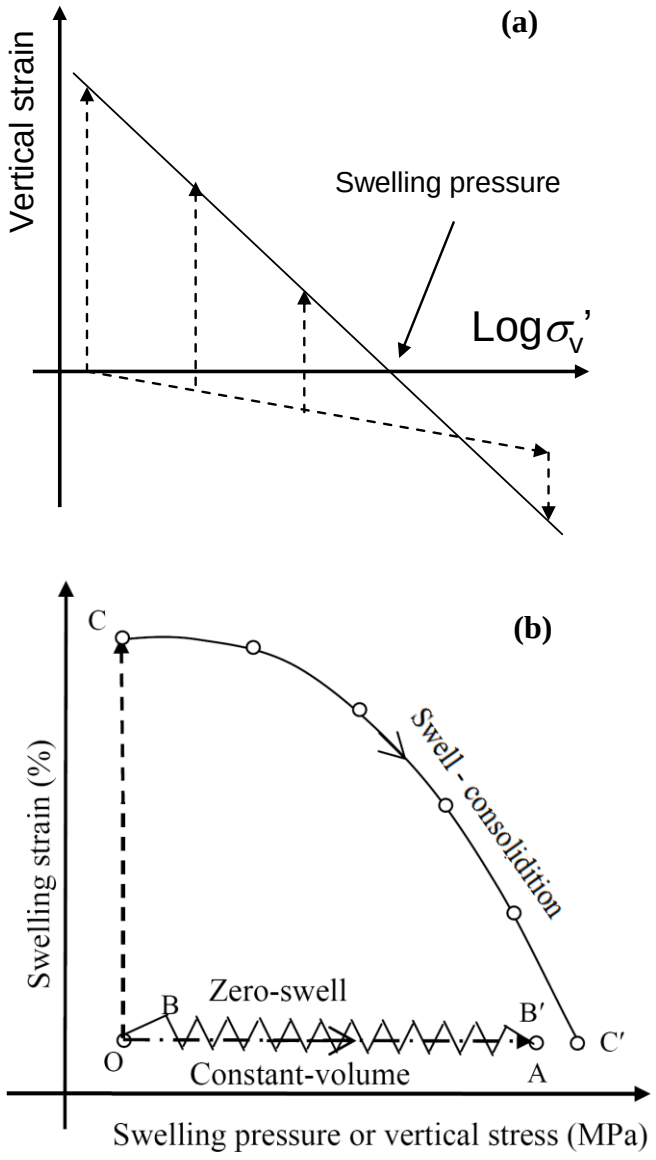

Figure 5. Methods for swelling pressure determination. (a) loading-wetting method, (b) constant-volume, zero-swell and swell-consolidation methods

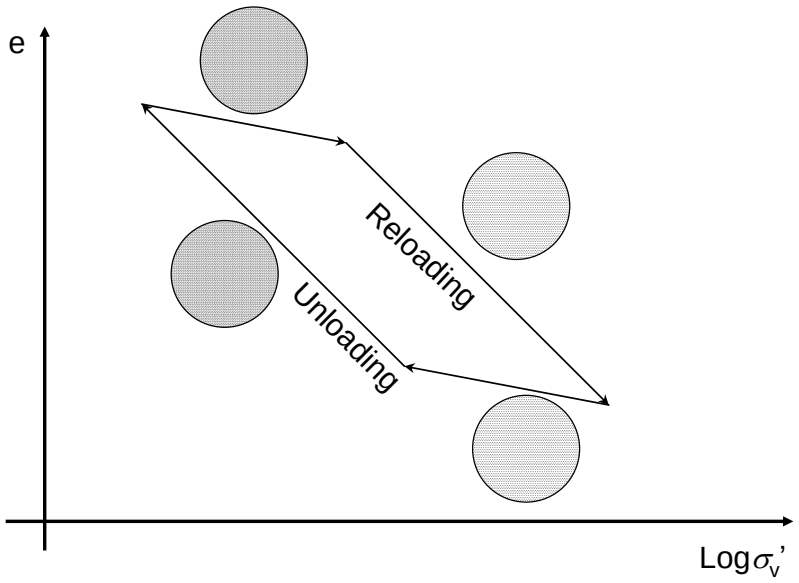

391

392

393 Figure 6. Representation of microstructure changes during unloading/reloading